Equalization and Precoding in Multi-User MIMO Relaying Systems and Their Diversity Bottleneck

Sebastian Stern, Yeicatl Ramos Vazquez and Robert F.H. Fischer
Institute of Communications Engineering, Ulm University, Ulm, Germany
Email: {sebastian.stern,robert.fischer}@uni-ulm.de

***Abstract*—In this paper, equalization and precoding in multi-user multiple-input/multiple-output (MIMO) relaying systems are considered. In particular, the user devices are connected to relays or small base stations which only cover small areas, so-called small cells. Via wireless backhaul, the relays are in turn connected to a central base station, forming a two-hop multi-user relaying system. It is shown how a naive realization of these relaying systems provokes a diversity bottleneck in the small cells, degrading the overall system performance. A strategy to prevent this bottleneck is proposed in combination with an antenna selection strategy for backhaul communication. Results obtained from numerical simulations are provided to complement the theoretical considerations. To this end, lattice-reduction-aided schemes are used to enable a full-diversity channel equalization.**

I. Introduction

Multi-user multiple-input/multiple-output (MIMO) transmission is one of the most promising techniques for future digital communication systems. In multi-user MIMO, several uncoordinated users transmit (or receive) their data—at the same time and the same frequency band—to (or from) one central base station. The uplink is called *MIMO multiple-access channel* and the downlink *MIMO broadcast channel*.

Actually, multi-user MIMO communication has become an attractive strategy with the introduction of *lattice-reduction-aided* (LRA) channel equalization [26], [23] for the uplink scenario. More precisely, LRA equalization enables a full-diversity MIMO detection [20] avoiding the enormous complexity of a maximum-likelihood detection [2]. In the sequel, LRA equalization was dualized to LRA preequalization or precoding [23], [24] via the uplink/downlink duality [21], [22].

Recently, the principle of so-called *small-cells* or *pico-cells* [1], [3], [15] has gained great interest. Thereby, the user devices aren't connected to one central base station covering a large area. Instead, the users communicate with one of several "small" base stations that cover a small range, e.g., only one building or one block of houses. All of these small base stations have to be connected to the core network. A possible approach for this is the *wireless backhaul*, i.e., the small base stations are supplied by one main base station via wireless connections. Certainly, the multi-user MIMO approach is suited for both small-cell and backhaul communication. We can interpret the combination of small cells and wireless backhaul as *multi-user MIMO relaying system*. Unfortunately, the literature on multi-user MIMO relaying systems, e.g., [6], [14], [4], is focused on linear or decision-feedback equalization as well as Tomlinson-Harashima precoding. All of these techniques are accompanied by a limitation to diversity order one.

In this paper, we consider the case were the small base stations are "smart": they act as joint receiver or transmitter for their allocated users; LRA techniques are employed to handle the multi-user interference and enable full diversity. In the same way, the small base station are supplied via a joint (LRA) receiver/transmitter at a central base station. Hence, in both "steps" of the transmission, we have to deal with a multi-user MIMO multiple-access or broadcast channel.

In particular, the related diversity orders in uplink and downlink transmission are discussed. A *diversity bottleneck* is identified which is present at the small base stations. We show how to avoid this bottleneck by choosing an appropriate number of antennas for small-cell and backhaul communication. A simple but effective antenna selection strategy is proposed for the case when not all of the available antennas are needed for transmission. The considerations are generalized to multi-hop relaying systems.

The paper is organized as follows: Sec. II reviews the MIMO multiple-access and broadcast channel model as well as LRA receiver- and transmitter-side equalization. Multi-user MIMO relaying systems are discussed in Sec. III and numerical results are provided in Sec. IV. The paper closes with a brief summary and conclusions in Sec. V.

II. Multi-User MIMO Transmission and Lattice-Reduction-Aided Equalization/Precoding

In this chapter, we review the essential concepts of both multi-user MIMO uplink and downlink transmission (*MIMO multiple-access channel* vs. *MIMO broadcast channel*). This especially includes the low-complexity full-diversity strategies of lattice-reduction-aided channel equalization or precoding.

A. System and Channel Model

We first have a closer look at the uplink and downlink multi-user MIMO scenario. In both cases, all signals are represented in discrete-time complex-baseband domain.[1]

This work has been supported by Deutsche Forschungsgemeinschaft (DFG) within the framework COIN under grant Fi 982/4-3.

[1]Notation: $\mathbb{F}_2$ denotes the Galois Field $\mathrm{GF}(2)$. The left pseudoinverse of an $U \times V$ matrix $\boldsymbol{A}$ is given by $\boldsymbol{A}^{+_\mathrm{l}} = (\boldsymbol{A}^\mathsf{H}\boldsymbol{A})^{-1}\boldsymbol{A}^\mathsf{H}$ for $U \geq V$ and the right pseudoinverse by $\boldsymbol{A}^{+_\mathrm{r}} = \boldsymbol{A}^\mathsf{H}(\boldsymbol{A}\boldsymbol{A}^\mathsf{H})^{-1}$ for $U \leq V$. The identity matrix is denoted as $\boldsymbol{I}$. Besides, we write $\boldsymbol{A}^{+_\mathrm{l}\mathsf{H}} = (\boldsymbol{A}^{+_\mathrm{l}})^\mathsf{H}$, $\boldsymbol{A}^{+_\mathrm{r}\mathsf{H}} = (\boldsymbol{A}^{+_\mathrm{r}})^\mathsf{H}$, and $\boldsymbol{A}^{-\mathsf{H}} = (\boldsymbol{A}^{-1})^\mathsf{H} = (\boldsymbol{A}^\mathsf{H})^{-1}$ if $U = V$.

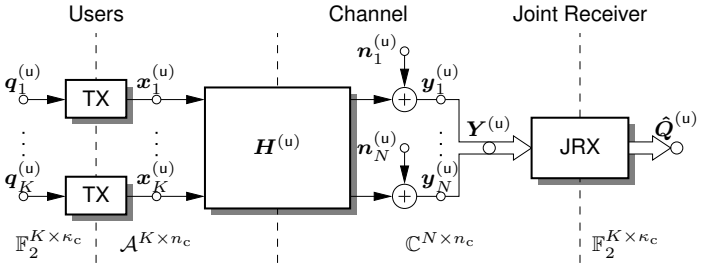

Fig. 1. System model of the MIMO multiple-access channel: K-user uplink transmission to a joint N-antenna receiver.

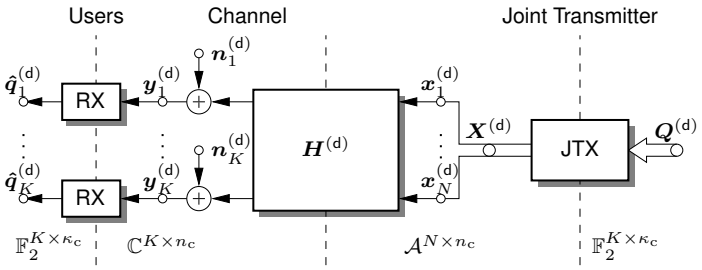

Fig. 2. System model of the MIMO broadcast channel: K-user downlink transmission from a joint N-antenna transmitter.

1) MIMO Multiple-Access Channel: The system model of the multi-user MIMO uplink scenario is illustrated in Fig. 1: K uncoordinated users transmit their data to one joint receiver (base station) equipped with $N \geq K$ antennas. We assume that the user devices have one single antenna.

In particular, each user wants to transmit a binary data stream which is separated into blocks of κ_c bits, denoted as row vectors $\boldsymbol{q}_1^{(\mathsf{u})}, \ldots, \boldsymbol{q}_K^{(\mathsf{u})}$. The transmitter (TX) processing is limited to the channel encoding (block code of rate R_c) and a mapping $\mathcal{M}$ from bits to signal points. More specifically, the signal points are drawn from a zero-mean constellation $\mathcal{A}$ with cardinality M and variance σ_a^2. They are combined into row vectors of transmit symbols $\boldsymbol{x}_1^{(\mathsf{u})}, \ldots, \boldsymbol{x}_K^{(\mathsf{u})}$ of length n_c (over time). Thus, in the uplink, the constellation points are directly radiated. In each block of n_c transmit symbols, $\kappa_\mathrm{c} = n_\mathrm{c} R_\mathrm{c} \log_2(M)$ data bits are represented.

The MIMO system equation is given by

$$\boldsymbol{Y}^{(\mathsf{u})} = \boldsymbol{H}^{(\mathsf{u})} \boldsymbol{X}^{(\mathsf{u})} + \boldsymbol{N}^{(\mathsf{u})} \,, \tag{1}$$

where all transmit vectors are combined into $\boldsymbol{X}^{(\mathsf{u})} \in \mathcal{A}^{K \times n_\mathrm{c}}$. The channel matrix $\boldsymbol{H}^{(\mathsf{u})} \in \mathbb{C}^{N \times K}$ is assumed to be constant over the block of n_c symbols. Its coefficients are assumed to be zero-mean i.i.d. complex Gaussian (block-fading channel). At each of the N receiving antennas, i.i.d. additive zero-mean white Gaussian noise with variance σ_n^2 is present. It is represented by the noise vectors $\boldsymbol{n}_1^{(\mathsf{u})}, \ldots, \boldsymbol{n}_N^{(\mathsf{u})}$ of length n_c which are combined into $\boldsymbol{N}^{(\mathsf{u})} \in \mathbb{C}^{N \times n_\mathrm{c}}$. The matrix $\boldsymbol{Y}^{(\mathsf{u})} \in \mathbb{C}^{N \times n_\mathrm{c}}$ contains the N vectors of n_c distorted receive symbols.

Via joint receiver (JRX) processing, the channel equalization and decoding are performed, resulting in K vectors of equalized and decoded symbols with length $k_\mathrm{c} = n_\mathrm{c} R_\mathrm{c}$. The vectors of the estimated $\kappa_\mathrm{c} = k_\mathrm{c} \log_2(M)$ bits, $\hat{\boldsymbol{q}}_1^{(\mathsf{u})}, \ldots, \hat{\boldsymbol{q}}_K^{(\mathsf{u})}$, are obtained by a demapping. They are jointly represented in $\hat{\boldsymbol{Q}}^{(\mathsf{u})} \in \mathbb{F}_2^{K \times \kappa_\mathrm{c}}$.

2) MIMO Broadcast Channel: Multi-user MIMO downlink transmission is similar to the uplink case, but it is performed in the reversed order (cf. Fig. 2): the base station acts as a joint transmitter (JTX) with N antennas to supply $K \leq N$ (single-antenna) user devices with their desired data streams.[2]

To this end, the K data streams are available at the transmitter. Again, we assume a block-wise coded transmission of κ_c bits per user that are combined into $\boldsymbol{Q}^{(\mathsf{d})} \in \mathbb{F}_2^{K \times \kappa_\mathrm{c}}$. An individual encoding with code rate R_c and a mapping to a signal constellation $\mathcal{A}$ is present. In contrast to the uplink, the K vectors of n_c signal points are (LRA) preequalized or precoded before radiation. This results in vectors of transmit symbols $\boldsymbol{x}_1^{(\mathsf{d})}, \ldots, \boldsymbol{x}_N^{(\mathsf{d})}$, combined into $\boldsymbol{X}^{(\mathsf{d})} \in \mathbb{C}^{N \times n_\mathrm{c}}$.

Similar to the uplink case, the MIMO system equation reads

$$\boldsymbol{Y}^{(\mathsf{d})} = \boldsymbol{H}^{(\mathsf{d})} \boldsymbol{X}^{(\mathsf{d})} + \boldsymbol{N}^{(\mathsf{d})} \,. \tag{2}$$

The (user/antenna) dimensions of the matrices are reversed when compared with (1), i.e., $\boldsymbol{H}^{(\mathsf{d})} \in \mathbb{C}^{K \times N}$, $\boldsymbol{N}^{(\mathsf{d})} \in \mathbb{C}^{K \times n_\mathrm{c}}$, and $\boldsymbol{Y}^{(\mathsf{d})} \in \mathbb{C}^{K \times n_\mathrm{c}}$. We assume the same statistical models as before (complex Gaussian channel and additive white Gaussian noise at the K receive antennas).[3] In the K uncoordinated receivers (RXs), the incoming blocks of noisy receive symbols, denoted as $\boldsymbol{y}_1^{(\mathsf{d})}, \ldots, \boldsymbol{y}_K^{(\mathsf{d})}$, are already equalized. Each user obtains its estimated block of bits, $\hat{\boldsymbol{q}}_1^{(\mathsf{d})}, \ldots, \hat{\boldsymbol{q}}_K^{(\mathsf{d})}$, by simply performing the channel decoding and demapping.

3) Signal-to-Noise Ratio: In order to express the signal-to-noise ratio (SNR), the transmitted energy per data bit in relation to the noise power spectral density

$$\frac{E_{\mathrm{b,TX}}}{N_0} = \frac{\sigma_a^2}{\sigma_n^2 R_\mathrm{c} \log_2(M)} \tag{3}$$

is a convenient measure for both the uplink and the downlink.

B. Lattice-Reduction-Aided Equalization

In order to handle the multi-user interference on the MIMO multiple-access or broadcast channel, several techniques have been proposed in the literature. First, simple linear equalization or preequalization can be employed. More advanced techniques are decision-feedback equalization (DFE) for the uplink or Tomlinson-Harashima precoding (THP) for the downlink [8], which utilize the principle of *successive interference cancellation* (SIC). However, all these strategies are not satisfactory since they only achieve diversity order one. In contrast, maximum-likelihood detection via the sphere decoder [2] or vector precoding [8], [13], [16] achieve the channel's diversity order, but with the price of a tremendous complexity.

Instead, LRA equalization or precoding are suited since they are low-complexity approaches providing full diversity [20]. In LRA equalization, the channel matrix is interpreted as

[2]As a consequence, the same infrastructure can be used to cover both the K-user multi-user uplink and downlink, e.g., via time or frequency duplex.

[3]The MIMO system equation is usually used as per-carrier model in multi-carrier schemes. Neglecting non-ideal behavior, e.g., from antennas or power amplifiers, $\boldsymbol{H}^{(\mathsf{d})} = (\boldsymbol{H}^{(\mathsf{u})})^{\mathsf{H}}$ is valid in case of a time-division duplex.

the generator matrix $\boldsymbol{G}$ of a lattice $\boldsymbol{\Lambda}(\boldsymbol{G})$. Via lattice-basis-reduction algorithms, a reduced basis is obtained, which is used for channel equalization. This approach lowers the noise or power enhancement in comparison to the equalization in the original basis, enabling a superior performance. We can divide the LRA schemes into LRA linear equalization or LRA DFE for the uplink [26], [23], and LRA linear preequalization or LRA (THP-type) precoding for the downlink [23], [24].

1) Receiver-Side Equalization: Again, we start with the uplink. For LRA equalization, it is advantageous to consider the lattice spanned by the $(N+K)\times K$ *augmented channel matrix* $\boldsymbol{\mathcal{H}}^{(\mathsf{u})} = \begin{bmatrix} \boldsymbol{H}^{(\mathsf{u})} \\ \sqrt{\zeta}\boldsymbol{I} \end{bmatrix}$, where $\zeta = \sigma_n^2/\sigma_a^2$ [25]. More specifically, the best performance is achieved if its dual lattice $\boldsymbol{\Lambda}((\boldsymbol{\mathcal{H}}^{(\mathsf{u})})^{+_{\mathrm{I}}\mathsf{H}})$ is reduced, i.e., the lattice defined by the *pseudoinverse of the augmented channel matrix* [10]. Then, the reduction task reads

$$\big(\boldsymbol{\mathcal{F}}^{(\mathsf{u})}\big)^{\mathsf{H}}\big(\boldsymbol{B}^{(\mathsf{u})}\big)^{-\mathsf{H}} = \big(\boldsymbol{\mathcal{H}}^{(\mathsf{u})}\big)^{+_{\mathrm{I}}\mathsf{H}}\big(\boldsymbol{Z}^{(\mathsf{u})}\big)^{-\mathsf{H}}\,, \qquad (4)$$

where the left part is the QR decomposition of the right part. The integer matrix $\boldsymbol{Z}^{(\mathsf{u})} \in \mathbb{G}^{K\times K}$ describes the change of basis; its elements are taken from the Gaussian integers $\mathbb{G} = \mathbb{Z} + \mathrm{j}\,\mathbb{Z}$ (*signal-point lattice* [8]). To this end, the signal constellation has to form a subset of $\mathbb{G}$ (optionally with an offset [23]), i.e., QAM ones are suited. The augmented *feedforward matrix* $\boldsymbol{\mathcal{F}}^{(\mathsf{u})} \in \mathbb{C}^{K\times(N+K)}$ has orthogonal rows; it transforms the (augmented) reduced channel into lower triangular structure. The lower triangular matrix $\boldsymbol{B}^{(\mathsf{u})} \in \mathbb{C}^{K\times K}$ with unit main diagonal describes the remaining causal interference.

Given (4), the LRA DFE receiver operates as depicted in Fig. 3: First, the matrix of receive symbols $\boldsymbol{Y}^{(\mathsf{u})}$ is linearly equalized via the feedforward matrix $\boldsymbol{F}^{(\mathsf{u})}$, called *non-integer equalization*.[4] The $K \times N$ left part of its augmented variant $\boldsymbol{\mathcal{F}}^{(\mathsf{u})}$ directly yields the matrix for minimum mean-square error (MMSE) linear equalization. Then, the SIC is performed: in decoding order $k = 1, \ldots, K$, the k^{th} row of $\tilde{\boldsymbol{Y}}^{(\mathsf{u})}$, denoted as $\tilde{\boldsymbol{y}}_k^{(\mathsf{u})}$, is (individually) decoded[5] to $\tilde{\boldsymbol{x}}_k^{(\mathsf{u})}$. To this end, the causal interference (previous $k-1$ rows of $\tilde{\boldsymbol{X}}$) is canceled via

$$\tilde{\boldsymbol{x}}_k^{(\mathsf{u})} = \mathrm{DEC}\big\{\tilde{\boldsymbol{y}}_k^{(\mathsf{u})} - \sum\nolimits_{l=1}^{k-1} \tilde{\boldsymbol{x}}_l^{(\mathsf{u})} b_{k,l}^{(\mathsf{u})}\big\}\,, \qquad (5)$$

where $\boldsymbol{B}^{(\mathsf{u})} = [\, b_{k,l}^{(\mathsf{u})}\,]$. The change of basis is reversed via $\boldsymbol{Z}^{(\mathsf{u})}$ (*integer equalization*). The matrix of estimated bits is obtained by a demapping of the symbols in $\hat{\boldsymbol{X}}^{(\mathsf{u})}$.

In order to solve the reduction task (4), the polynomial-time CLLL algorithm can be employed [11]. In particular, the *(C)LLL with deep insertions* [9] is suited, since the related integer matrix $\boldsymbol{Z}^{(\mathsf{u})}$ incorporates a decoding order close to the V-BLAST one [12]. For the details see [9].

2) Transmitter-Side Equalization: For the downlink, the reduction task (4) has to be adapted to [19]

$$\big(\boldsymbol{B}^{(\mathsf{d})}\big)^{-\mathsf{H}}\big(\boldsymbol{\mathcal{F}}^{(\mathsf{d})}\big)^{\mathsf{H}} = \big(\boldsymbol{Z}^{(\mathsf{d})}\big)^{-\mathsf{H}}\big(\boldsymbol{\mathcal{H}}^{(\mathsf{d})}\big)^{+_{\mathrm{r}}\mathsf{H}}\,, \qquad (6)$$

[4]In case of LRA linear equalization, the feedback part in Fig. 3 is inactive ($\boldsymbol{B}^{(\mathsf{u})} = \boldsymbol{I}$) and $\boldsymbol{\mathcal{F}}^{(\mathsf{u})}_{\mathrm{linear}} = (\boldsymbol{B}^{(\mathsf{u})})^{-1}\boldsymbol{\mathcal{F}}^{(\mathsf{u})}$, i.e., both factors of the QR decomposition are incorporated in the feedforward matrix.

[5]In case of uncoded transmission, the channel decoding is just a simple quantization with respect to $\mathbb{G}$.

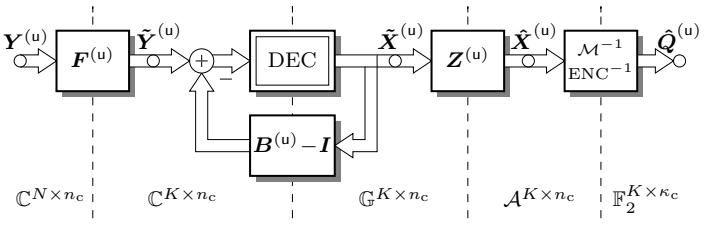

Fig. 3. Receiver model of LRA decision-feedback equalization. In case of LRA linear equalization, the feedback part is turned off ($\boldsymbol{B}^{(\mathsf{u})} = \boldsymbol{I}$).

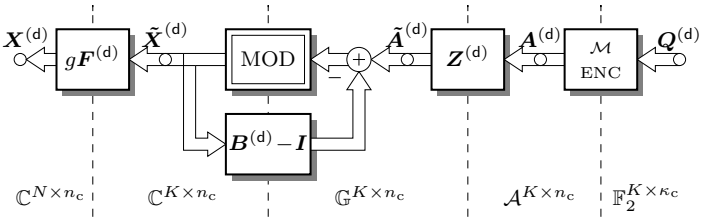

Fig. 4. Transmitter model of LRA (THP-type) precoding. In case of LRA linear preequalization, the feedback part is turned off ($\boldsymbol{B}^{(\mathsf{d})} = \boldsymbol{I}$).

where the left part is now the RQ decomposition of the right part. The $K \times (N + K)$ augmented channel is defined by $\boldsymbol{\mathcal{H}}^{(\mathsf{d})} = \big[\boldsymbol{H}^{(\mathsf{d})}\ \sqrt{\zeta}\boldsymbol{I}\big]$. Again, $\boldsymbol{B}^{(\mathsf{d})} \in \mathbb{C}^{K\times K}$ is lower triangular with unit main diagonal, and $\boldsymbol{Z}^{(\mathsf{d})} \in \mathbb{G}^{K\times K}$. However, the augmented feedforward matrix $\boldsymbol{\mathcal{F}}^{(\mathsf{d})} \in \mathbb{C}^{(N+K)\times K}$ now has orthogonal columns instead of rows.[6]

In comparison to the uplink case, the LRA precoder operates in reversed order as illustrated in Fig. 4: First, the matrix of encoded and mapped data symbols $\boldsymbol{A}^{(\mathsf{d})}$ is linearly preequalized via $\boldsymbol{Z}^{(\mathsf{d})}$, i.e., the integer equalization is performed. Following this, we have a SIC similar to (5), where for $k = 1, \ldots, K$, $\tilde{\boldsymbol{x}}_k^{(\mathsf{u})}$ and $\tilde{\boldsymbol{y}}_k^{(\mathsf{u})}$ are replaced by $\tilde{\boldsymbol{x}}_k^{(\mathsf{d})}$ and $\tilde{\boldsymbol{a}}_k^{(\mathsf{d})}$, respectively, and $\boldsymbol{B}^{(\mathsf{d})} = [\, b_{k,l}^{(\mathsf{d})}\,]$. Besides, a symbol-wise *modulo operation* with respect to the *precoding lattice* [8] is present instead of decoding. To this end, the signal constellation not only has to form a subset of $\mathbb{G}$ (optionally with an offset), but it additionally has to be *periodically extendable*.[7] The last step before radiation is the MMSE linear non-integer equalization[8] via the $N\times K$ upper part $\boldsymbol{F}^{(\mathsf{d})}$ of $\boldsymbol{\mathcal{F}}^{(\mathsf{d})}$. The channel-dependent factor g is set to meet the power constraint $N\sigma_x^2 = K\sigma_a^2$.

Noteworthy, at the (individual) receivers, the transmitter-side modulo operation leads to signal points that are modulo-congruent to the ones of the signal constellation $\mathcal{A}$. For uncoded transmission, it is sufficient to perform the modulo operation in the receivers once again. In the coded case, a *nearest-neighbor decoding* is realized, cf. [8], [18].

[6]For that purpose, reduction algorithms that are defined to operate on columns have to be adapted to work on rows instead. Alternatively, the algorithms for the uplink can can be used for $\boldsymbol{\Lambda}((\boldsymbol{\mathcal{H}}^{(\mathsf{d})})^{+_{\mathrm{r}}})$, then, however, resulting in an *upper triangular* matrix $\boldsymbol{B}^{(\mathsf{d})}$ (reversed encoding order).

[7]For example, square-QAM constellations fulfill this requirement. In that case, the modulo operation is given by $\mathrm{MOD}\{z\} = z - \sqrt{M}\mathcal{Q}_{\mathbb{G}}\{z/\sqrt{M}\}$, $z \in \mathbb{C}$, where M is the cardinality and $\mathcal{Q}_{\mathbb{G}}\{z\} = \lfloor \mathrm{Re}\{z\} \rceil + \mathrm{j}\,\lfloor \mathrm{Im}\{z\} \rceil$.

[8]If LRA linear preequalization is used instead, the feedback part in Fig. 4 is inactive ($\boldsymbol{B}^{(\mathsf{d})} = \boldsymbol{I}$) and $\boldsymbol{\mathcal{F}}^{(\mathsf{d})}_{\mathrm{linear}} = \boldsymbol{\mathcal{F}}^{(\mathsf{d})}(\boldsymbol{B}^{(\mathsf{d})})^{-1}$, i.e., both factors of the RQ decomposition are incorporated in the feedforward matrix.

III. Multi-User MIMO Relaying Systems and Their Diversity Order in Uplink and Downlink

On the basis of the full-diversity techniques of LRA equalization or precoding, we are able to consider the diversity orders (asymptotic slope of the error-rate curves) of different multi-user transmission scenarios. Besides the standard scenario of single-hop transmission, we are interested in two-hop scenarios, where the user devices are allocated to several so-called *small base stations* (SBSs) or *relays*. Via a joint *wireless backhaul* these SBSs are, in turn, supplied by one main base station (MBS).

A. Single-Hop Transmission

We first consider the diversity order of a single-hop multi-user transmission, where K individual user devices are directly supplied by one central MBS with $N \geq K$ antennas.

In Fig. 5, the respective uplink transmission is illustrated. We have the standard MIMO multiple-access scenario with $\boldsymbol{H}^{(\mathrm{u})} \in \mathbb{C}^{N \times K}$. As the JRX at the MBS performs LRA linear or decision-feedback equalization, the error curves exhibit the diversity order

$$D_{\mathrm{single}} = N \ . \tag{7}$$

The related K-user downlink transmission is simply obtained by replacing the JRX at the MBS with an N-antenna JTX performing LRA linear preequalization or precoding (cf. Fig. 1 vs. Fig. 2). Then, each user has an individual RX, and $\boldsymbol{H}^{(\mathrm{d})} \in \mathbb{C}^{K \times N}$. The diversity is exactly the same as in the uplink case, i.e., (7) is valid for the uplink and downlink.

In the example of Fig. 5, we have $N = K = 4$, and hence $D_{\mathrm{single}} = 4$ for both uplink and downlink transmission.

B. Two-Hop Transmission via Relay Stations

We continue with the two-hop multi-user scenario. In particular, we consider relaying systems as illustrated in Fig. 6. For the sack of clarity we first restrict our considerations to uplink processing. They will subsequently be transferred to downlink transmission.

Again, we denote the total number of users in the system as K. They, however, do not directly communicate with the MBS any more. Instead, each user device is allocated to one of the ρ_{S} SBSs or relays, which are responsible for several users within their area of supply. To be exact, the numbers of users read $K_{\mathrm{S},s}$, $s = 1, \ldots, \rho_{\mathrm{S}}$. In the example of Fig. 6, the two devices on top are allocated to SBS 1, whereas the two users at the bottom are allocated to SBS 2, i.e., $\rho_{\mathrm{S}} = 2$ and $K_{\mathrm{S},1} = K_{\mathrm{S},2} = 2$. All SBSs share the wireless backhaul in order to transmit the uplink data from their users to the MBS.

More specifically, we assume that the SBSs and their users do not interfere with each other, i.e., multi-user interference is only present among the users allocated to one specific SBS. In the same way, the communication via the wireless backhaul does not interfere with the links between users and SBSs and vice versa.[9] The transmission model at hand is very suited for the *small-cell* scenario discussed in the introduction.

[9]To this end, we can separate the different links via time-division or frequency-division multiple access.

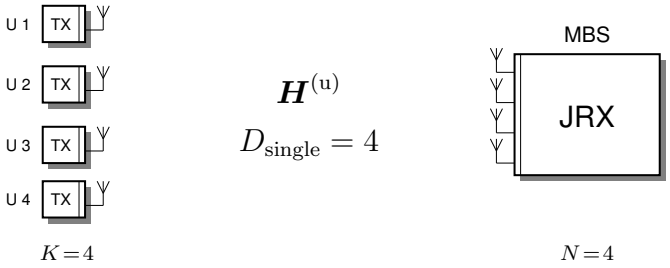

Fig. 5. Single-hop multi-user MIMO uplink scenario: $K = 4$ users are directly connected to MBS with $N = 4$ antennas. The related single-hop downlink scenario is obtained by replacing the JRX at the MBS with a JTX, and each individual TX at the user devices with an individual RX.

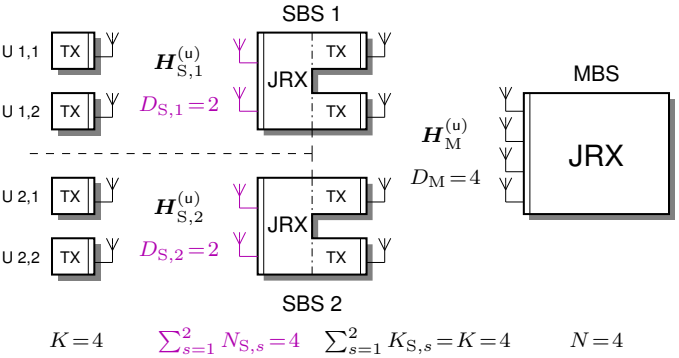

Fig. 6. Two-hop multi-user MIMO uplink scenario with $K = 4$ users: each of the $\rho_{\mathrm{s}} = 2$ SBSs supplies $K_{\mathrm{S},1} = K_{\mathrm{S},2} = 2$ users. The SBSs are connected to one MBS with $N = 4$ antennas via multi-user wireless backhaul. The SBSs have $N_{\mathrm{S},1} = N_{\mathrm{S},2} = 2$ antennas to communicate with their allocated users; their number of antennas for backhaul connection is the number of allocated users. The diversity bottleneck is marked violet. The related two-hop downlink scenario is obtained by replacing each JRX at the MBS and the SBSs with a JTX, and each individual TX at the user devices and the SBSs with an individual RX.

1) Multi-User Processing: In the SBSs/relays, we consider the *decode-and-forward* strategy: all incoming signals are decoded and all outgoing are re-encoded.

In particular, as illustrated in Fig. 6, the SBSs serve as JRX for their allocated users, i.e., one separate MIMO multiple-access channel is present per SBS. In order to be able to handle the small-cell multi-user interference via LRA equalization, $N_{\mathrm{S},s} \geq K_{\mathrm{S},s}$, $s = 1, \ldots, \rho_{\mathrm{S}}$, antennas are needed at the SBSs. The channels are described by $\boldsymbol{H}^{(\mathrm{u})}_{\mathrm{S},s} \in \mathbb{C}^{N_{\mathrm{S},s} \times K_{\mathrm{S},s}}$. In the example of Fig. 6, we have $N_{\mathrm{S},1} = N_{\mathrm{S},2} = 2$ (the numbers of users per small cell).

Since the multi-user wireless backhaul is shared among the *uncoordinated SBSs*, only the MBS can act as a JRX, cf. Fig. 6. Each SBS has to posses at least $K_{\mathrm{S},s}$ independent transmitters (and related antennas) to be able to handle all data streams of their allocated users. We assume that this number is exactly $K_{\mathrm{S},s}$ to enable a (standard) LRA equalization. As the MBS thus has to receive $K = \sum_{s=1}^{\rho_{\mathrm{S}}} K_{\mathrm{S},s}$ independent data streams, its number of antennas must be $N \geq K$ (just like in the single-hop scenario, the relays are just "inserted" in between, cf. Fig. 5). The multi-user wireless backhaul is described via $\boldsymbol{H}^{(\mathrm{u})}_{\mathrm{M}} \in \mathbb{C}^{N \times K}$. In Fig. 6, we have $N = K = 4$, and two independent streams per SBS ($K_{\mathrm{S},1} = K_{\mathrm{S},2} = 2$).

2) Diversity Order and Bottleneck: In the following, we will take a closer look at the diversity order obtained by the multi-user MIMO relaying systems at hand.

We first restrict to the case where $N_{\mathrm{S},s} = K_{\mathrm{S},s} = K/\rho_{\mathrm{S}}$, $s = 1, \ldots, \rho_{\mathrm{S}}$, and $N = K$. We thus have the same number of users at each of the SBSs and all channel matrices are square ones. As illustrated in Fig. 6, the total number of antennas in every "step" of the uplink transmission is

$$K = \sum\nolimits_{s=1}^{\rho_{\mathrm{S}}} N_{\mathrm{S},s} = \sum\nolimits_{s=1}^{\rho_{\mathrm{S}}} K_{\mathrm{S},s} = N \,. \tag{8}$$

As a consequence, one might think that the diversity order of the (whole) relaying system reads $D_{\mathrm{relay}} = N$. Indeed, the wireless backhaul transmission has diversity order $D_{\mathrm{M}} = N$, since its multi-user processing is equivalent to the single-hop case (cf. Fig. 5). In contrast, a *diversity bottleneck* is present at the SBSs (marked violet in Fig. 6): even though we have the total number of N receive antennas for small-cell communication, the joint multi-user processing is restricted to N/ρ_{S} antennas per SBS. Hence, in the small cells, we only have the diversity order $D_{\mathrm{S},1} = \ldots, D_{\mathrm{S},\rho_{\mathrm{S}}} = N/\rho_{\mathrm{S}}$. Since the diversity order (and the related performance) of the whole relaying system is determined by its poorest link(s),

$$\begin{aligned} D_{\mathrm{relay}} &= \min\left\{D_{\mathrm{M}}, D_{\mathrm{S},1}, \ldots, D_{\mathrm{S},\rho_{\mathrm{S}}}\right\} && (9)\\ &= \min\left\{N, N_{\mathrm{S},1}, \ldots, N_{\mathrm{S},\rho_{\mathrm{S}}}\right\}, && (10) \end{aligned}$$

where the bottleneck is marked violet. For a naive realization of a multi-user relaying system according to Fig. 6 this means

$$D_{\mathrm{relay,naive}} = \min\left\{N, \frac{N}{\rho_{\mathrm{S}}}, \ldots, \frac{N}{\rho_{\mathrm{S}}}\right\} = \frac{N}{\rho_{\mathrm{S}}} \,, \tag{11}$$

i.e., the diversity order is inversely proportional to the number of SBSs ρ_{S}. Applying (11) to our example in Fig. 6 with $K = N = 4$ and $\rho_{\mathrm{S}} = 2$, we only achieve diversity order two, thus half the diversity compared with (7) and Fig. 5.

For the general case where $N > K$ and/or $N_{\mathrm{S},s} > K_{\mathrm{S},s}$, the situation is similar: The MBS is responsible for all K user-data streams within the whole relaying system, whereas the SBSs only have to supply a subset of the users. Consequently, the number of antennas at the MBS will usually be chosen to be much higher than those of the SBSs, provoking the violet-marked diversity bottleneck in (10).

3) Prevention of the Diversity Bottleneck: The diversity bottleneck degrades the transmission performance of multi-user MIMO relaying systems when compared with the direct (single-hop) multi-user scenario. Nevertheless, it is possible to avoid the bottleneck with the strategy depicted in Fig. 7 (changes in comparison to Fig. 6 are marked blue).

In particular, each of the SBSs generally has to possess N (receive) antennas for its small-cell communication, i.e., $N_{\mathrm{S},s} = N$, $s = 1, \ldots, \rho_{\mathrm{S}}$. The channel matrices describing the small-cell uplink are extended to $\boldsymbol{H}_{\mathrm{S},s}^{(\mathrm{u})} \in \mathbb{C}^{N \times K_{\mathrm{S},s}}$. The rest of the relaying system stays the same; the backhaul transmission is performed with $K_{\mathrm{S},s}$ antennas per SBS (equivalent to number of allocated users) as before.

The diversity order of the small-cell connections then reads $D_{\mathrm{S},s} = N_{\mathrm{S},s} = N \; \forall s$. Since $D_{\mathrm{M}} = N$ is still valid, we have

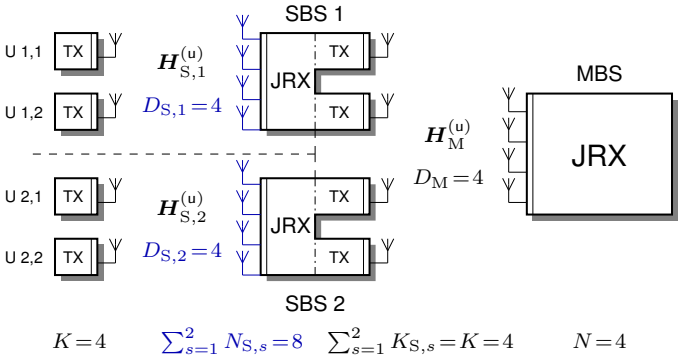

Fig. 7. Two-hop multi-user MIMO uplink transmission strategy for $K = 4$ users avoiding the diversity bottleneck of Fig. 6: at the SBSs, the number of (small-cell) receive antennas is increased to $N_{\mathrm{S},1} = N_{\mathrm{S},2} = N = 4$ (marked blue). Small cells and wireless backhaul share the same diversity.

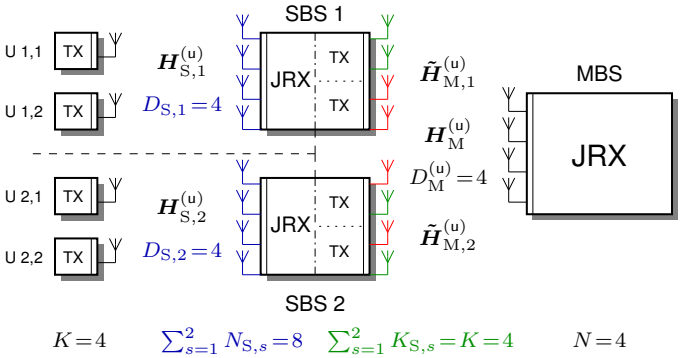

Fig. 8. Two-hop multi-user MIMO uplink transmission strategy of Fig. 7 including antenna selection: at each of the SBSs, $N_{\mathrm{S},1} = N_{\mathrm{S},2} = N = 4$ antennas are available for backhaul communication. $K_{\mathrm{S},1} = K_{\mathrm{S},2} = 2$ of them are active (green); the other two antennas per SBS are idle (red).

$D_{\mathrm{relay}} = \min\{N, N, \ldots, N\} = N$ according to (10) and the bottleneck is removed ($D_{\mathrm{relay}} = D_{\mathrm{single}} = N$, cf. (7)). This, however, is achieved at the expense of a large increase in the total number of small-cell receive antennas. More precisely,

$$\sum\nolimits_{s=1}^{\rho_{\mathrm{S}}} N_{\mathrm{S},s} = \rho_{\mathrm{S}} \cdot N \tag{12}$$

antennas are needed (directly proportional to ρ_{S}). As visible in Fig. 7, in our example it is doubled from four to eight in comparison to the other "steps" of transmission where only four antennas are present. In turn, the diversity is doubled from two to four when compared with the naive approach and we have the same order as in the single-hop case in Fig. 5.

The total number of antennas described in (12) may become very large if relaying systems with many SBSs and users are present. In order to avoid high cost, a trade-off between the complete prevention of the diversity bottleneck and the number of antennas is possible by choosing $K_{\mathrm{S},s} < N_{\mathrm{S},s} < N$.

4) Antenna Selection in Case of Bottleneck Prevention: If the bottleneck-preventing relaying strategy of Fig. 7 is employed, $N_{\mathrm{S},s} = N > K_{\mathrm{S},s}$ antennas are used for small-cell communication at the SBSs, but $K_{\mathrm{S},s}$ antennas are sufficient for the wireless backhaul. If the same antenna infrastructure is taken for both purposes, e.g., in case of a time-division duplex, we have a surplus of antennas for the backhaul links.

The respective uplink scenario is depicted in Fig. 8. In our example, we have to choose $K_{\mathrm{S},s} = 2$ active antennas at each SBS for the backhaul uplink (marked green in Fig. 8); the other $N_{\mathrm{S},s} - K_{\mathrm{S},s} = 2$ ones are idle (marked red).

Still the question remains how to choose the active antennas for each SBS. To this end, we can employ a simple but effective *heuristic antenna selection strategy*: For each SBS $s = 1, \ldots, \rho_{\mathrm{S}}$, the channel gains/coefficients for the links between the $N_{\mathrm{S},s}$ available antennas and the N antennas at the MBS are considered. They are combined into the matrices $\tilde{\boldsymbol{H}}_{\mathrm{M},s}^{(\mathrm{u})} \in \mathbb{C}^{N \times N_{\mathrm{S},s}}$. In order to "predict" each antenna's performance, the column norms of $\tilde{\boldsymbol{H}}_{\mathrm{M},s}^{(\mathrm{u})}$ are suited since they reflect the receive energy (at the MBS). More specifically, we have to consider the squared norms $\|\tilde{\boldsymbol{h}}_{\mathrm{M},s,n}^{(\mathrm{u})}\|_2^2$, $n = 1, \ldots, N_{\mathrm{S},s}$, where $\tilde{\boldsymbol{h}}_{\mathrm{M},s,n}^{(\mathrm{u})}$ denotes the n^{th} column of $\tilde{\boldsymbol{H}}_{\mathrm{M,s}}^{(\mathrm{u})}$.

The active antennas are selected as follows: we sort the $N_{\mathrm{S},s}$ (squared) norms in descending order. In this way, the indexes of the first $K_{\mathrm{S},s}$ norms represent the antennas with the strongest links; they are activated to communicate with the MBS. The other $N_{\mathrm{S},s} - K_{\mathrm{S},s}$ antennas are inactive. Noteworthy, the $K_{\mathrm{S},s}$ columns with largest squared norms are directly included into the final channel matrix $\boldsymbol{H}_{\mathrm{M}}^{(\mathrm{u})}$. It represents the wireless backhaul with respect to all activated antennas.

5) Downlink Transmission: The above considerations can be transferred to the K-user downlink scenario. Utilizing the relationship between both cases (cf. Fig. 1 vs. Fig. 2), this is achieved by replacing each individual TX with an individual RX, and each JRX with a JTX in Fig. 6. The number of receive antennas is transferred into the number of transmit antennas, and vice versa. Then, a MIMO broadcast channel is present in each small cell, where the SBSs supply their $K_{\mathrm{S},s}$ user devices with their data via $N_{\mathrm{S},s} \geq K_{\mathrm{S},s}$ transmit antennas. The MBS acts as JTX with $N \geq K$ antennas to transmit all K data streams to the SBSs, i.e., the backhaul is a MIMO broadcast channel where each SBS has $K_{\mathrm{S},s}$ receive antennas.

In the naive realization of the multi-user MIMO downlink relaying system, we choose $N_{\mathrm{S},s} = K_{\mathrm{S},s}$ antennas for small-cell supply at the SBSs. This provokes the same diversity bottleneck (11) as for uplink communication, with the only difference that we have *transmit* instead of *receive* antennas. We are able to avoid the bottleneck by choosing $N_{\mathrm{S},s} = N$ transmit antennas per SBS, yielding—in accordance with Fig. 7—the same diversity in every step of the relaying system. This, however, increases the total number of *transmit antennas* at the SBSs to (12). Hence, all aspects hold (in a transferred sense) for both the uplink and the downlink scenario.

In conformity with Fig. 8, a surplus of (backhaul) *receive antennas* at the SBSs may be present for the downlink. Then, we can apply the above antenna-selection strategy to the related downlink matrices. It, however, has to be adapted to work on the $N_{\mathrm{S},s}$ squared *row norms* of $\tilde{\boldsymbol{H}}_{\mathrm{M},s}^{(\mathrm{d})} \in \mathbb{C}^{N_{\mathrm{S},s} \times N}$, $s = 1, \ldots, \rho_{\mathrm{S}}$, as they reflect the receive power (at the SBSs). In particular, per SBS, the $K_{\mathrm{S},s}$ largest row norms are chosen and combined into the final backhaul matrix $\boldsymbol{H}_{\mathrm{M}}^{(\mathrm{d})} \in \mathbb{C}^{K \times N}$.

C. Multi-Hop Transmission via Cascades of Relay Stations

We can generalize our theoretical considerations from the two-hop to the multi-hop scenario. Then, a hierarchical structure of SBSs is present above the user level. As an example, comparing a three-hop scenario with our two-hop scenario of Fig. 6, "low-level" SBSs are inserted between the user level and the present "top-level" SBSs; the top-level SBSs supply the low-level ones. However, a diversity bottleneck is always present as long as one single SBS does not possess the same number of (small-cell) antennas as the MBS—independently from the hierarchical degree. Moreover, our proposed antenna selection strategy is suited for SBSs of all hierarchical levels.

IV. Numerical Results

We complement the theoretical aspects of Sec. III with results obtained from numerical simulations. In particular, we address the multi-user MIMO relaying scenario of Fig. 6 with the total number of $K = 4$ users in the system, $\rho_{\mathrm{S}} = 2$ SBSs (two users per SBSs), and $N = 4$ antennas at the MBS. In accordance with (3), we assume that the same SNR is present for each user and hop.[10] All simulations have been performed with a large number of channels and noise samples according to Sec. II.

We have a closer look at both LRA linear equalization and LRA DFE (uplink), and both LRA linear preequalization and LRA precoding (downlink). The reduction tasks (4) or (6) are solved via the (C)LLL with deep insertions ($\delta = 0.75$). We restrict to MMSE non-integer linear equalization (augmented matrices). For the sake of clarity we apply the same equalization scheme in all SBSs and the MBS (e.g., LRA DFE in every JRX and LRA precoding in every JTX).

A. Uncoded Transmission

We first consider uncoded transmission since the diversity order directly becomes apparent in the related error curves.

1) Uplink: We start with the uplink. In Fig. 9, the bit-error rate (BER) of 16QAM transmission is shown in dependency of $E_{\mathrm{b,TX}}/N_0$ in dB (averaged over all bit streams at the MBS).

Restricting to LRA linear equalization (top), the impact of the diversity bottleneck is clearly visible ($N_{\mathrm{S},s} = 2$; Fig. 6). More precisely, nearly the same error rate as for single-hop two-user transmission is present ($N = K = 2$; diversity order two). In the low-SNR regime, we additionally see a degradation of the relaying system due to the effect of error propagation (symbol with wrong decision in SBS is forwarded to MBS). The bottleneck is completely avoided when choosing $N_{\mathrm{S},s} = 4$ (strategy according to Fig. 7; diversity order four). In that case, the curve is very close to the one for four-user single-hop transmission (again, a little loss is present due to error propagation). A trade-off between bottleneck prevention and increase in the total number of small-cell antennas is achieved

[10] Given the assumption that the noise power at the RX antennas is always the same and $E_{\mathrm{b,TX}}$ is kept constant, the *total transmit power* of the two-hop system is doubled when compared with the single-hop one, cf. Fig. 5 vs. Fig. 6. Since we want to focus on the impact of the diversity bottleneck in comparison to the single-hop case, we consider the error curves in dependency of $E_{\mathrm{b,TX}}$ per user and hop. If the total TX power is of interest instead, we can simply shift the curves for two-hop transmission 3 dB to the right.

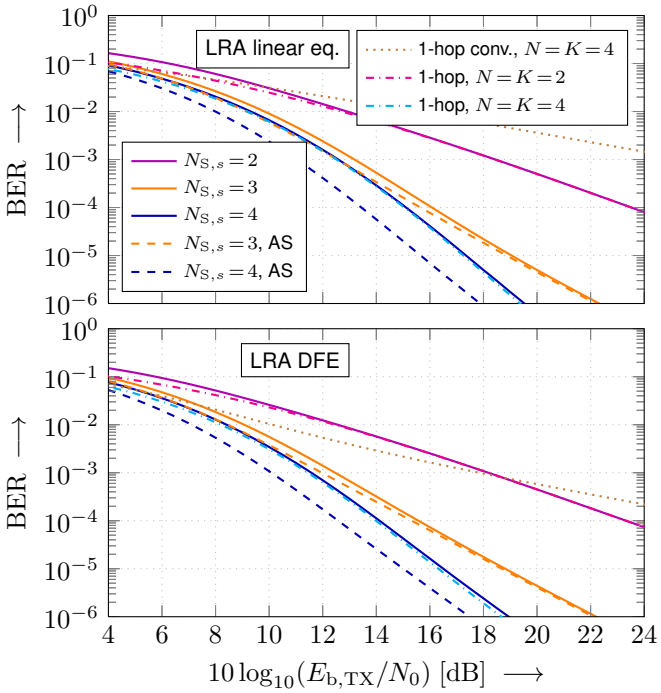

Fig. 9. BER of uncoded 16QAM two-hop multi-user uplink transmission (Gray labeling). $\rho_{\mathrm{S}} = 2$ SBSs with two allocated users, i.e., $K = 4$ users in the system. $N = 4$ antennas at the MBS. Variation of the number of (small-cell) antennas $N_{\mathrm{S},s}$ per SBS with or without antenna selection (AS). Top: LRA linear equalization. Bottom: LRA DFE. Lattice reduction according to (4) (MMSE variant). For comparison, the curves for single-hop LRA transmission and conventional linear equalization/DFE (conv.) are given.

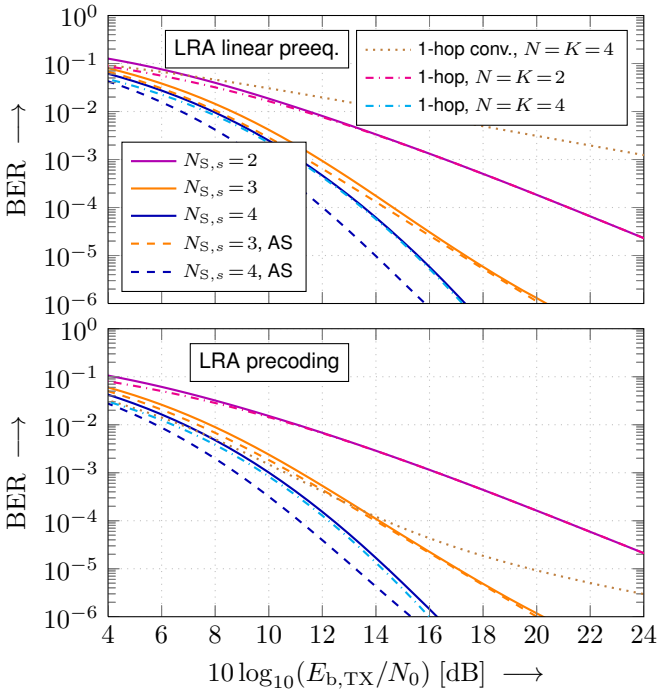

Fig. 10. BER of uncoded 16QAM two-hop multi-user downlink transmission (Gray labeling). $\rho_{\mathrm{S}} = 2$ SBSs with two allocated users, i.e., $K = 4$ users in the system. $N = 4$ antennas at the MBS. Variation of the number of (small-cell) antennas $N_{\mathrm{S},s}$ per SBS with or without antenna selection (AS). Top: LRA linear preequalization. Bottom: LRA precoding. Lattice reduction according to (6) (MMSE variant). For comparison, the curves for single-hop LRA transmission and conventional linear equalization/THP (conv.) are given.

by choosing three antennas per SBS (diversity order three). Noteworthy, conventional (non-LRA) linear equalization only achieves diversity one even for $N = K = 4$. If antenna selection (AS) is active; we see an additional gain in SNR of about 1.5 dB for the case $N_{\mathrm{S},s} = 4$ (scenario of Fig. 8), whereas the diversity order stays the same. It even outperforms the (standard) single-hop transmission with four users. For the case $N_{\mathrm{S},s} = 3$, the positive impact is distinctly lowered.

Considering the curves for LRA DFE instead (Fig. 9), we can mainly draw the same conclusions as above. The curves for diversity two and three are slightly moved to the left in comparison to the top of Fig. 9. For both single- and two-hop transmission with diversity order four, we have a gain of about 0.5–1 dB. Hence, the principle of SIC becomes more advantageous as the diversity order increases. For conventional (non-LRA) DFE, a flattening to diversity order one is clearly visible even in case of four-user single-hop transmission.

2) Downlink Transmission: We continue with the BER of the related downlink in Fig. 10 (16QAM; averaged over all users) to see if the same behavior as in the uplink is present.

Indeed, the naive relaying approach ($N_{\mathrm{S},s} = 2$) only achieves diversity order two. In contrast, the bottleneck-preventing strategy ($N_{\mathrm{S},s} = 4$) again enables diversity order four just like in case of four-user single-hop downlink transmission. A further gain in SNR of about 1.5 dB is possible when AS is active. By choosing $N_{\mathrm{S},s} = 3$, a trade-off between diversity and the number of antennas is enabled. Conventional linear preequalization only achieves diversity one. In general, LRA linear preequalization exhibits a gain of about 2 dB when compared with LRA linear (receiver-side) equalization.

Contrasting LRA linear preequalization and LRA precoding (Fig. 10 bottom), again we see a significant gain of precoding only for the curves with diversity order four. Besides, a gain of roughly 2 dB is present in comparison to LRA (receiver-side) DFE. Conventional THP performs better than conventional DFE, but the flattening to diversity order one is still present.

B. Coded Transmission

Finally, we consider coded transmission. In the uncoded case, the same conclusions could be drawn for the uplink and downlink scenario as well as for LRA linear (non-integer) equalization vs. SIC. In the coded case, we hence exemplify the downlink scenario with LRA precoding. As already mentioned above, we apply the decode-and-forward strategy: the signals are decoded and re-encoded in the SBSs.

In particular, we apply bit-interleaved coded modulation (BICM) [5] with respect to the low-density parity-check (LDPC) code and interleaver defined in the DVB-S2 standard [7]. A soft-decision decoding via belief-propagation (50 iterations) is performed. The bit-log-likelihoods are extracted the from the modulo-congruent signal points (cf. Sec. II) via nearest-neighbor approximation with respect to the (Gray-labeled) constellation points [8], [17], [18].

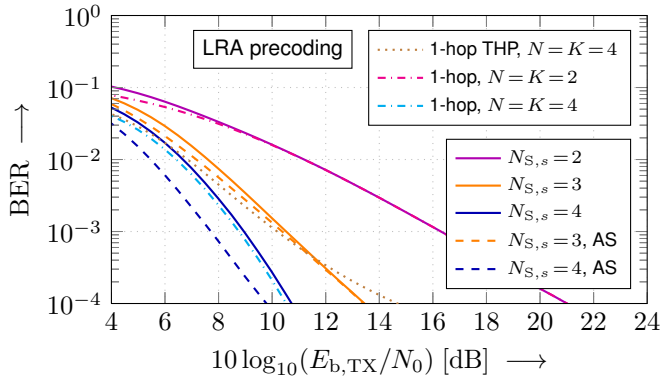

Fig. 11. BER of coded 64QAM two-hop multi-user downlink transmission (Gray labeling; code rate $R_{\mathrm{c}}=2/3$). $\rho_{\mathrm{S}}=2$ SBSs with two allocated users, i.e., $K=4$ users in the system. $N=4$ antennas at the MBS. Variation of the number of (small-cell) antennas $N_{\mathrm{S},s}$ per SBS with or without antenna selection (AS). LRA precoding according to (6) (MMSE variant). The curves for single-hop LRA precoding and conventional THP are given.

In Fig. 11, the simulation results for code rate $R_{\mathrm{c}}=2/3$ in combination with a 64QAM constellation are shown. Thus, the same information rate (4 bits/symbol) as in Fig. 10 is present. We see that the diversity order of all curves roughly stays the same when compared with the uncoded ones in Fig. 10. The reason for that is the individual channel coding *over time* for the block-fading channel at hand. Noteworthy, *space-time-coding* is not possible as a joint decoding cannot be performed. Instead of a diversity gain, a gain in SNR (*coding gain*) up to about 1 dB is present at $\mathrm{BER}=10^{-3}$ ($N_{\mathrm{S},s}=4$ with AS).

All theoretical aspects with respect to the diversity order are still valid for the coded case. This especially concerns the diversity bottleneck and its prevention: the two-hop transmission with only $N_{\mathrm{S},s}=2$ (small-cell) antennas nearly shows the same performance as the two-user single-hop one. Avoiding the bottleneck by choosing $N_{\mathrm{S},s}=4$, we achieve diversity order four just like in case of the four-user single-hop scenario. Conventional THP exhibits a suitable performance in the low-SNR regime, but flattens out if the SNR is increased.

V. Summary and Conclusions

Multi-user MIMO relaying systems have been considered in both uplink and downlink. To this end, the full-diversity techniques of lattice-reduction-aided equalization or precoding have been employed. A diversity bottleneck has been identified at the relays, which can be avoided by increasing the number of antennas for small-cell communication. For the case when the relays use the same number of antennas in the small cell and backhaul, an antenna selection strategy has been proposed.

Simulation results for the example of two relays with two allocated users have revealed that the theoretical considerations hold in practice. Besides, the derivations are not only generally valid for two-hop relaying systems, but they can be generalized to (hierarchical) multi-hop relaying systems.

Future research could deal with the adaptation of the scenarios at hand to other channel models beyond the i.i.d. Gaussian one, or the improvement of the antenna selection strategy.

References

[1] 3GPP. *TR36.932 (V12.0.0): Scenarios and Requirements of LTE Small Cell Enhancements for E-UTRA and E-UTRAN (Release 12)*, Dec. 2012.

[2] E. Agrell, T. Eriksson, A. Vardy, K. Zeger. Closest Point Search in Lattices. *IEEE Trans. Inf. Theory* **48** (8), pp. 2201–2214, Aug. 2002.

[3] A. Bleicher: A Surge in Small Cells. *IEEE Spectrum* **50** (11), pp. 38–39, Jan. 2013.

[4] Y. Cai, R.C. de Lamare, L.L. Yang, M. Zhao. Robust MMSE Precoding Based on Switched Relaying and Side Information for Multiuser MIMO Relay Systems. *IEEE Trans. Vehic. Techn.*, **64** (12), pp. 5677–5687, Dec. 2015.

[5] G. Caire, G. Taricco, E. Biglieri. Bit-Interleaved Coded Modulation. *IEEE Trans. Inf. Theory* **43** (3), pp. 927–946, May 1998.

[6] C.B. Chae, T. Tang, R.W. Heath Jr., S. Cho. MIMO Relaying With Linear Processing for Multiuser Transmission in Fixed Relay Networks. *IEEE Trans. Signal Process.*, **56** (2) pp. 727–738, Feb. 2008.

[7] European Telecommunications Standards Institute. DVB-S2. *ETSI Standard EN 302 307 V1.1.1: Digital Video Broadcasting (DVB)*, 2005.

[8] R.F.H. Fischer. *Precoding and Signal Shaping for Digital Transmission*. Wiley-IEEE Press, 2002.

[9] R.F.H. Fischer. Complexity-Performance Trade-Off Algorithms for Combined Lattice-Reduction and QR decomposition. *Int. Journal of Electronic and Commun. (AEÜ)*, **66**, pp. 871–879, 2012.

[10] R.F.H. Fischer, M. Cyran, S. Stern. Factorization Approaches in Lattice-Reduction-Aided and Integer-Forcing Equalization. *Int. Zurich Seminar on Commun.*, Zurich, Switzerland, Mar. 2016.

[11] Y.H. Gan, C. Ling, W.H. Mow. Complex Lattice Reduction Algorithm for Low-Complexity Full-Diversity MIMO Detection. *IEEE Trans. Signal Process.*, **57** (7) pp. 2701–2710, July 2009.

[12] G.D. Golden, G.J. Foschini, *et al.* Detection Algorithm and Initial Laboratory Results Using V-BLAST Space-Time Communication Architecture. *Electronics Letters*, pp. 14–15, Jan. 1999.

[13] B.M. Hochwald, C.B. Peel, A.L. Swindlehurst. A Vector-Perturbation Technique for Near-Capacity Multi-Antenna Multi-User Communication. Part II: Perturbation. *IEEE Trans. Commun.* **53** (3), pp. 537-544, Mar. 2005.

[14] S. Jang, J. Yang, D.K. Kim. Minimum MSE Design for Multiuser MIMO Relay. *IEEE Commun. Letters* **14** (9), pp. 812-812, Sep. 2010.

[15] T. Nakamura et al. Trends in Small Cell Enhancements in LTE Advanced. *IEEE Commun. Magazine* **51** (2), pp. 98–105, Feb. 2013.

[16] D.A. Schmidt, M. Joham, W. Utschick. Minimum Mean Square Error Vector Precoding. *Int. Symp. on Personal, Indoor and Mobile Radio Commun.*, pp. 107–111, Sept. 2005.

[17] S. Stern, R.F.H. Fischer. Lattice-Reduction-Aided Precoding for Coded Modulation over Algebraic Signal Constellations. *20th Int. ITG Workshop on Smart Antennas)*, pp. 356–363, Munich, Germany, Mar. 2016.

[18] S. Stern, R.F.H. Fischer. Joint Algebraic Coded Modulation and Lattice-Reduction-Aided Preequalization. *Electronics Letters* **52** (7), pp. 523–525, Apr. 2016.

[19] S. Stern and R.F.H. Fischer. Advanced Factorization Strategies for Lattice-Reduction-Aided Preequalization. *IEEE Int. Symp. on Inf. Theory*, pp. 1471–1475, Barcelona, Spain, July 2016.

[20] M. Taherzadeh, A. Mobasher, A.K. Khandani. LLL Reduction Achieves the Receive Diversity in MIMO Decoding. *IEEE Trans. Inf. Theory* **53** (12), pp. 4801–4805, Dec. 2007.

[21] P. Viswanath, D.N.C. Tse. Sum Capacity of the Vector Gaussian Broadcast Channel and Uplink-Downlink Duality. *IEEE Trans. Inf. Theory* **49** (8), pp. 1912–1921, Aug. 2003.

[22] S. Vishwanath, N. Jindal, A. Goldsmith. Duality, Achievable Rates, and Sum-Rate Capacity of Gaussian MIMO Broadcast Channels. *IEEE Trans. Inf. Theory* **49** (10), pp. 2658–2668, Oct. 2003.

[23] C. Windpassinger, R.F.H. Fischer. Low-Complexity Near-Maximum-Likelihood Detection and Precoding for MIMO Systems using Lattice Reduction. *IEEE Inf. Theory Workshop*, Paris, France, pp. 345–348, Mar. 2003.

[24] C. Windpassinger, R.F.H. Fischer, J.B. Huber. Lattice-Reduction-Aided Broadcast Precoding. *IEEE Trans. Commun.* **52** (12), pp. 2057–2060, Dec. 2004.

[25] D. Wübben, R. Böhnke, V. Kühn, K.D. Kammeyer. Near-Maximum-Likelihood Detection of MIMO Systems using MMSE-Based Lattice Reduction. *IEEE Int. Conf. on Commun.*, pp. 798–802, June 2004.

[26] H. Yao, G.W. Wornell. Lattice-Reduction-Aided Detectors for MIMO Communication Systems. *IEEE Global Telecomm. Conf.*, Nov. 2002.